Birefringence, Deformation, and Scattering of Segmentally Flexible Macromolecules under an External Agent. Steady-State Properties in an Electric Field

ARTICLE *in* THE JOURNAL OF PHYSICAL CHEMISTRY B · SEPTEMBER 1999

Impact Factor: 3.3 · DOI: 10.1021/jp9910385

Birefringence, Deformation, and Scattering of Segmentally Flexible Macromolecules under an External Agent. Steady-State Properties in an Electric Field

B. Carrasco, F. G. Díaz, M. C. López Martínez, and J. García de la Torre*

Departamento de Química Física, Universidad de Murcia, 30071 Murcia, Spain

Received: March 26, 1999; In Final Form: June 9, 1999

Segmentally flexible macromolecules are composed of a few rigid subunits joined by semiflexible joints. When such macromolecules are exposed to an external agent, they become oriented and deformed, and this fact can be monitored by birefringence and scattering. In this paper, we present a theoretical treatment of deformation and scattering of segmentally flexible macromolecules in an external agent that complements existing treatments of birefringence. We treat in detail the case in which the external agent is an electric field, particularizing for the case of a macromolecule with two cylindrically symmetric subunits. We focus on the steady-state behavior of the molecule in the field, studying the effect of arbitrarily high field strengths, which can be simulated using a Monte Carlo procedure. We show how the dependence of birefringence and deformation on field strength can be related to the electrooptical properties of the macromolecule and its flexibility. Particular attention is paid to macromolecular deformation expressed in term of the gyration tensor, whose components can be determined from separate scattering experiments with different scattering geometries. A joint discussion of deformations and birefringence provides a nexus between the techniques of electric birefringence and electric-field light scattering.

Introduction

Polar and polarizable macromolecules in solution can be oriented by an electric field, and the macromolecular solution then becomes birefringent or dichroic due to the orientation of the solute. The degree of ordering in the electric field, as manifested by the electric dichroism or birefringence, is a source of information on electrooptical and conformational properties of the macromolecule. If the electric field is suddenly removed, the birefringence or dichroism decays to the field-off value, and the rate of this dynamic process is a further source of information on macromolecular structure and dynamics. The essential aspects of these techniques are described in some monographs.[1,2] When the macromolecule behaves as a rigid body, both the steady-state and the transient behavior are known. For bodies of arbitrary shape, the theory of Holcomb and Tinoco[3] allows the prediction of the field-on, static properties. The birefringence or dichroism decay can be predicted from the theory of Wegener et al.[4] along with methods[5−7] for rotational relaxation times.

Other external agents are similarly able to orient (and eventually deform) macromolecules in solution. That is the case if the solution is submitted to shear, elongational, or other types of flow, for which, in addition to the effect of the macromolecule on the viscosity and other rheological properties of the solution, the macromolecule itself suffers effects that can be measured and related to its structure, flexibility, etc.

The birefringence and, to a lesser extent, the deformation or scattering of macromolecules under external agents such as fields or flows is only well understood when the macromolecule complies with some very simple, extreme models; for instance, when it behaves as a completely flexible random coil, or as a completely rigid particle. However, a situation which is not adequately solved is that of semiflexible macromolecules, and particularly for those of a special type, usually called segmentally flexible macromolecules, using a term coined by Stryer and co-workers,[8] which are the subject of study in the present work. Segmentally flexible macromolecules are constituted by a few rigid subunits or domains, joined by more or less flexible hinges or joints. A typical case is that of broken-rod macromolecules, having two rodlike arms, such as the myosin rod is sometimes supposed to be[9,10] or some specially prepared synthetic polypeptides.[11,12] Whole myosin,[9,13] myosin filament,[14,15] and immunoglobulins[16] are more complex examples, with more subunits and joints. A rigorous and general description of the electrooptics of these macromolecules is very difficult since the aspects of conformational flexibility, interaction with the electric field, and segmental mobility are intricately interwoven. Moreover, there are cases, like the electrical birefringence study of the myosin structural dynamic by Eden and Highsmith,[17] where it is unclear whether one is observing continuous joint flexibility or a field-induced conformational change between discrete conformations.

The behavior of segmentally flexible macromolecules under an electric field and, in general, under any external agent (which may also be, for instance, a shear or elongational flow) presents two aspects; one of them regards the properties of the macromolecule in its steady state, when that agent has been applied for a sufficiently long time, and the other is the time evolution of the properties when the agent is switched on or off. The second aspect is particularly complex, because in addition to the molecule−field interaction and its effect on macromolecular conformation, one has to include in the treatment a description of the macromolecular hydrodynamics. Leaving the latter aspect for a separate work, we describe in this paper the steady-state properties.

The interaction of macromolecules with external agent is characterized usually in terms of the birefringence or dichroism induced in the macromolecular solution by the orientation of

* To whom correspondence should be addressed. email: jgt@fcu.um.es.

10.1021/jp9910385 CCC: $18.00
Published on Web 08/31/1999

the segments or subunits. Furthermore, a frequent simplifying assumption is to make the external field very weak, so that the perturbation in the conformational statistics of the macromolecule is very small. Under a very weak electric field, the steady-state, field-on electrooptic properties are then given by the Kerr law.[1] The calculation of Kerr constants of semiflexible macromolecules can be done analytically with ease.[18] The cases of moderate or even rather high fields present difficulties, both in the realization of experiments and in the formulation of theories, and are seldom considered. However, it is in those cases when the interplay between the field effects and the limited flexibility of the macromolecule becomes more evident. Therefore, important information about the structure and flexibility of the macromolecule can be extracted from properties in strong fields.

While the theoretical study of the behavior of macromolecules under external forces or fields of arbitrary strength presents notable difficulties, it is quite simple to predict such behavior using simulation. For steady-state behavior, a useful tool is Monte Carlo simulation which has already been employed in an early work from our laboratory to simulate electric birefringence.[19] As we shall describe later, that work is further developed in the present study.

Although birefringence (and similarly dichroism) is the property most often studied in this context, another effect of the external agent is to deform the macromolecule, altering its conformational statistics and therefore changing its overall dimensions. Such changes could be monitored by scattering of light or other electromagnetic radiation. Indeed, the technique of electric-field light scattering has been experimentally investigated,[20,21] although it is not in widespread use. Light scattering in flows is also an interesting possibility.[22,23] In any case, scattering intensity changes reflect the change in the distribution of conformations. In this paper we have developed a theoretical formalism for describing the deformation and scattering intensities in the case of segmentally flexible macromolecules. We also obtain interesting relationships between the overall particle deformation probed by scattering and the orientation of segments probed by electric birefringence.

As commented above, the efficiency of the external field to deform or orient the macromolecule depends jointly on the field strength and the degree of flexibility. Therefore, the study of those effects as a function of field strength should provide valuable information on the structure of segmentally flexible macromolecules (or continuous bending macromolecules[24]). In order to illustrate this with numerical results, we study the properties (electric birefringence or dichroism, as well as deformation and scattering) of a simplified model with two subunits in an electric field. The two-subunit model represents well the main general features of segmental flexibility and is also very useful for a variety of biological systems[19,25] (for a review see García de la Torre[26]).

Theory

In this section we formulate quantities that express the degree of deformation of the macromolecular structure developing a novel framework to describe the instantaneous or average conformation in terms of the gyration tensor. Later, relationships with scattering and birefringence will be obtained. This treatment extends and completes the results presented in former works.[19,27−29] The derivations in this section will be valid not only for electric fields but also for any other external agents, like a flow.

Deformation in the Presence of External Agents. In the absence of external agents, any possible conformation of the particle, independent of the rigidity or flexibility of the structure, can have any orientation in space. The gyration tensor is isotropic: it takes a diagonal form, with components

$$\langle G\rangle_{\alpha\alpha,0} = {}^1/_3\langle s^2\rangle_0 \tag{1}$$

$$\langle G\rangle_{\alpha\beta,0} = 0 \qquad \alpha \neq \beta \tag{2}$$

with

$$\langle s^2\rangle_0 = \sum f_i(\langle d_i^2\rangle_0 + s_i^2) \tag{3}$$

where $\langle ...\rangle_0$ indicates average (both orientational and conformational) in the absence of field, s^2 is the squared radius of gyration, s_i^2 defines the same parameter for each subunit, f_i is the mass fraction of subunit i, and d_i is the distance from the center of mass of the whole particle to the center of the ith subunit.

Under the action of the field the molecule is deformed and its average dimensions are modified. The change in the radius of gyration can be expressed[29] in terms of a deformation ratio

$$\delta^2 = \frac{\langle s^2\rangle - \langle s^2\rangle_0}{\langle s^2\rangle_0} \tag{4}$$

δ^2 is the change in $\langle s^2\rangle$ relative to its unperturbed value.

Similarly, we extend this definition to the diagonal components of the gyration tensor, whose changes are referred to their unperturbed values, so that

$$\delta_{\alpha\alpha}{}^2 = \frac{\langle G^2\rangle_{\alpha\alpha} - {}^1/_3\langle s^2\rangle_0}{{}^1/_3\langle s^2\rangle_0} \tag{5}$$

Then, it follows from eqs 4 and 5 that

$$\delta^2 = {}^1/_3(\delta_{xx}{}^2 + \delta_{yy}{}^2 + \delta_{zz}{}^2) \tag{6}$$

In most cases of practical interest, the external agent acts along a given direction (say, axis Z), and the perpendicular directions (axes X and Y) are equivalent. Such happens for orientation in an electric field, or in shear or axial elongational flow. In those circumstances, $\delta_{xx}{}^2 = \delta_{yy}{}^2$.

Average Value of the Gyration Tensor. Here we present the general treatment to obtain the average value of the gyration tensor for a particle composed of rigid subunits of arbitrary shape for any range of segmental flexibility.

The gyration tensor is defined as

$$\langle \mathbf{G}\rangle = \left\langle \frac{1}{m}\int_v \mathbf{ss}\,\rho(\mathbf{s})\,d\tau \right\rangle \tag{7}$$

For a flexible particle, the average $\langle ...\rangle$ (which would be unnecessary for a rigid particle) must be carried out over all the conformations that the particle may adopt. In eq 7, $\mathbf{s}$ is, for an instantaneous conformation, the position vector of a point within the particle with respect to its instantaneous center of mass, and $\mathbf{ss}$ is the tensor with Cartesian components $\mathbf{ss}_{\alpha\beta} = s_\alpha s_\beta$, where $\alpha,\beta = x,y,z$. The particle center is defined so that

$$\int_v \mathbf{s}\,\rho(\mathbf{s})\,d\tau = \mathbf{0} \tag{8}$$

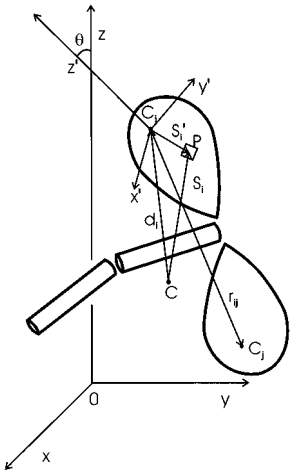

Figure 1. Schematic representation of a multisubunit, segmentally flexible macromolecule, showing the laboratory axes (*X*, *Y*, *Z*), the subunit axes (*X*′, *Y*′, *Z*′), and the centers of mass of each subunit (C_i, C_j) and the whole particle (*C*). Some other elements shown are: $\mathbf{d}_i$, the vector from C to C_i; $\mathbf{s}_i$, the position vector of a point *P* within the particle with respect to *C*; $\mathbf{s}'_i$, the position vector of any point within subunit *i*, with respect to C_i; $\mathbf{r}_{ij}$, the vector from C_i and C_j.

for a given conformation. The integration is carried out over the volume, *V*, occupied by the particle in its instantaneous conformation. $\rho(\mathbf{s})$ is density at point $\mathbf{s}$; the type of density will depend on the type of radiation scattering used to monitor the size and conformation of the particle. In any case, we define

$$m = \int_v \rho(\mathbf{s})\, d\tau \tag{9}$$

Sometimes it will be valid to take $\rho(\mathbf{s})$ equal or proportional to the mass density; then, *m* in eq 9 will be the true mass of the particle. Furthermore, in many applications density will be uniform, and $\rho(\mathbf{s})$ will be just a constant, $\rho = m/V$.

It can be demonstrated that the gyration tensor has an alternative expression, formulated in terms of the distances $\mathbf{r}_{12} = \mathbf{r}_2 - \mathbf{r}_1$, between every pair of points, with position vectors $\mathbf{r}_1$ and $\mathbf{r}_2$ with respect to an arbitrary origin (not necessarily the particle's center):

$$\langle \mathbf{G} \rangle = \left\langle \frac{1}{2m^2} \int_v \int_v \mathbf{r}_{12}\mathbf{r}_{12}\, \rho(\mathbf{r}_1)\rho(\mathbf{r}_2)\, d\tau_1\, d\tau_2 \right\rangle \tag{10}$$

We consider now that the particle is actually composed of N_s rigid segments or subunits, connected by joints which are more or less flexible. Looking separately at the individual subunits, an expression similar to eq 7 can be formulated for each of them

$$\langle \mathbf{G}_i \rangle = \left\langle \frac{1}{m_i} \int_{v_i} \mathbf{s}'_i \mathbf{s}'_i\, \rho(\mathbf{s}'_i)\, d\tau \right\rangle \tag{11}$$

Now, $\mathbf{s}'_i$ is the position vector of any point within subunit *i*, with respect to the center of this subunit, C_i (see Figure 1). We may write $\mathbf{s}'_i = \mathbf{s}_i - \mathbf{d}_i$. Furthermore, we express $\mathbf{s}'_i$ and $\langle \mathbf{G}_i \rangle$ in eq 11 in some adequately chosen system of axes fixed in that subunit.

Then, our problem is the calculation of the whole particle's $\langle \mathbf{G} \rangle$ from the individual $\langle \mathbf{G}_i \rangle$ of each subunit. After a lengthy but straightforward derivation, we arrive at the following result:

$$\langle \mathbf{G} \rangle = \sum_{i=1}^{N_s} f_i (\langle \mathbf{d}_i \mathbf{d}_i \rangle + \langle \mathbf{A}_i^{\mathrm{T}} \cdot \mathbf{G}_i \cdot \mathbf{A}_i \rangle) \tag{12}$$

where $\mathbf{A}_i$ is the matrix which transforms vectors in the lab-fixed system into the subunit-fixed system of axes. The superscript T in eq 12 indicates matrix transposition. In eq 12 the center of mass has to be evaluated first. It can be shown that there is an alternative formulation in which the first term in the right-hand side of eq 12 is replaced by another that depends on the distance vectors, $\mathbf{r}_{ij}$, between the centers of mass of the subunits. Thus, the expression for $\langle \mathbf{G} \rangle$ reads

$$\langle \mathbf{G} \rangle = \frac{1}{2} \sum_{i=1}^{N_s} \sum_{j=1}^{N_s} f_i f_j \langle \mathbf{r}_{ij} \mathbf{r}_{ij} \rangle + \sum_{i=1}^{N_s} f_i \langle \mathbf{A}_i^{\mathrm{T}} \cdot \mathbf{G}_i \cdot \mathbf{A}_i \rangle \tag{13}$$

which is a generalization of the results for the radius of gyration obtained by Solvez et al.[27]

According to eq 12, $\langle \mathbf{G} \rangle$ has two contributions, one from the distances of the subunits to the center of mass and another from the gyration tensor of the subunits.

Pointlike Subunits. As presented in previous work,[28,29] if the subunits were pointlike the second term would be negligible and we would have a gyration tensor

$$\langle \mathbf{G}' \rangle = \frac{1}{N} \sum_{i=1}^{N_s} \langle \mathbf{d}_i \mathbf{d}_i \rangle \tag{14}$$

A practical case where this situation holds is that of a chainlike structure composed of many subunits of identical (or similar) sizes. Then, for most subunits the distances d_i^2 will be greater than their individual radius of gyration, G_i is much smaller that $\mathbf{d}_i\mathbf{d}_i$, and eq 14 is practically valid. For a gyration tensor evaluated as in eq 14, deformation parameters δ'^2 or $\delta'_{\alpha\alpha}{}^2$ can be defined as in eqs 4 and 5, using $\mathbf{G}'$ in place of $\mathbf{G}$.

Axially Symmetric Subunits. In the case of nonpoint-like subunits, with a given size and shape, we have to add the contribution arising from changes in $\langle \mathbf{A}_i^{\mathrm{T}} \cdot \mathbf{G}_i \cdot \mathbf{A}_i \rangle$. An important and practically useful case is that in which the shapes of the subunits have axial symmetry, as indicated above. Then, the subunit gyration tensors are diagonal, with only two distinct components:

$$\mathbf{G}_i = \begin{pmatrix} G_i^{\perp} & 0 & 0 \\ 0 & G_i^{\perp} & 0 \\ 0 & 0 & G_i^{\parallel} \end{pmatrix} \tag{15}$$

For an elongated shape, such as a prolate ellipsoid or a long rod, $G_i^{\parallel} > G_i^{\perp}$ while for an oblate ellipsoid, or a disk, $G_i^{\parallel} < G_i^{\perp}$. $G_i^{\parallel}$ and $G_i^{\perp}$ measure, respectively, the spread of mass along the axial and perpendicular direction.

Furthermore, a set of two polar angles $\{\theta,\phi\}$ suffices to express the orientation of the subunits. Expressing the transformation matrix in terms of the polar angles, the components

of the tensor $\mathbf{A}_i^{\mathrm{T}}\cdot\mathbf{G}_i\cdot\mathbf{A}_i$ can be written as

$$(\mathbf{A}_i^{\mathrm{T}}\cdot\mathbf{G}_i\cdot\mathbf{A}_i)_{xx} = G_i^{\perp}(\cos^2\phi_i + \cos^2\theta_i \sin^2\phi_i) + G_i^{\parallel}\sin^2\theta_i \sin^2\phi_i \quad (16a)$$

$$(\mathbf{A}_i^{\mathrm{T}}\cdot\mathbf{G}_i\cdot\mathbf{A}_i)_{xy} = (G_i^{\perp} - G_i^{\parallel})\sin^2\theta_i \sin\phi_i \cos\phi_i \quad (16b)$$

$$(\mathbf{A}_i^{\mathrm{T}}\cdot\mathbf{G}_i\cdot\mathbf{A}_i)_{xz} = (G_i^{\parallel} - G_i^{\perp})\sin\theta_i \cos\theta_i \sin\phi_i \quad (16c)$$

$$(\mathbf{A}_i^{\mathrm{T}}\cdot\mathbf{G}_i\cdot\mathbf{A}_i)_{yy} = G_i^{\perp}(\sin^2\phi_i + \cos^2\theta_i \cos^2\phi_i) + G_i^{\parallel}\sin^2\theta_i \cos^2\phi_i \quad (16d)$$

$$(\mathbf{A}_i^{\mathrm{T}}\cdot\mathbf{G}_i\cdot\mathbf{A}_i)_{yz} = (G_i^{\perp} - G_i^{\parallel})\sin\theta_i \cos\theta_i \cos\phi_i \quad (16e)$$

$$(\mathbf{A}_i^{\mathrm{T}}\cdot\mathbf{G}_i\cdot\mathbf{A}_i)_{zz} = G_i^{\perp}\sin^2\theta_i + G_i^{\parallel}\cos^2\theta_i \quad (16f)$$

In this case, eq 12 can be further developed. The z axes are taken as the symmetry axis and the electric field direction, respectively, for the subunit-fixed and lab-fixed systems. The first polar angle, θ, is that defined by these two directions, and it is statistically distributed according to the subunit−field interaction. The other angle does not take part in the interaction energy, and therefore its distribution is uniformly random. Then, carrying out the orientational averages according to the indicated distributions, we arrive at the final result that this product is, like $\mathbf{G}_i$, a diagonal matrix, with

$$\langle\mathbf{A}_i^{\mathrm{T}}\cdot\mathbf{G}_i\cdot\mathbf{A}_i\rangle_{\alpha\beta} = 0 \quad \alpha \neq \beta \quad (17a)$$

$$\langle\mathbf{A}_i^{\mathrm{T}}\cdot\mathbf{G}_i\cdot\mathbf{A}_i\rangle_{xx} = \langle\mathbf{A}_i^{\mathrm{T}}\mathbf{G}_i\mathbf{A}_i\rangle_{yy} = {}^1/_2[G_i^{\perp} + G_i^{\parallel} + \langle\cos^2\theta_i\rangle(G_i^{\perp} - G_i^{\parallel})] \quad (17b)$$

$$\langle\mathbf{A}_i^{\mathrm{T}}\cdot\mathbf{G}_i\cdot\mathbf{A}_i\rangle_{zz} = G_i^{\perp} - \langle\cos^2\theta_i\rangle(G_i^{\perp} - G_i^{\parallel}) \quad (17c)$$

At this point, it is important to make some checks on the results in eq 17. We note that $\mathrm{Tr}\langle\mathbf{A}_i^{\mathrm{T}}\cdot\mathbf{G}_i\cdot\mathbf{A}_i\rangle = 2G_i^{\perp} + G_i^{\parallel} = \mathrm{Tr}(\mathbf{G}_i)$ as it should since the trace is an invariant.

One particular situation of interest is when all the subunits are spherical. Then the subunit gyration tensor is isotropic, identically in the subunit-fixed and in the lab-fixed systems; the diagonal components are all equal to $\sigma_i^2/5$, so that

$$\langle\mathbf{A}_i^{\mathrm{T}}\cdot\mathbf{G}_i\cdot\mathbf{A}_i\rangle = (\sigma_i^2/5)\mathbf{I} \quad (18)$$

where σ_i is the radius of the subunit. We recall that the square radius of gyration for the individual spherical subunits is $3\sigma_i^2/5$.

The other particularly interesting situation is when the subunits are rods of length L_i and diameter d_i. Then, $G_i^{\parallel} = L_i^2/12$ and $G_i^{\perp} = d_i/16$, with $s_i^2 = L_i^2/12 + d_i^2/8$. If they are sufficiently long, $L_i^2 \gg d_i^2$, $G_i^{\parallel} \gg G_i^{\perp}$, and we may simplify the result:

$$\langle\mathbf{A}_i^{\mathrm{T}}\cdot\mathbf{G}_i\cdot\mathbf{A}_i\rangle_{xx} = \langle\mathbf{A}_i^{\mathrm{T}}\cdot\mathbf{G}_i\cdot\mathbf{A}_i\rangle_{yy} = {}^1/_2G_i^{\parallel}(1 - \langle\cos^2\theta_i\rangle) \quad (19a)$$

$$\langle\mathbf{A}_i^{\mathrm{T}}\cdot\mathbf{G}_i\cdot\mathbf{A}_i\rangle_{zz} = G_i^{\parallel}\langle\cos^2\theta_i\rangle \quad (19b)$$

In the absence of fields, θ is uniformly distributed, with $\langle\cos^2\theta\rangle = 1/3$ in eq 17, so that the tensor $\langle\mathbf{A}_i^{\mathrm{T}}\mathbf{G}_i\mathbf{A}_i\rangle_0$ is, as it should be, diagonal and isotropic, with diagonal elements

$$\langle\mathbf{A}_i^{\mathrm{T}}\cdot\mathbf{G}_i\cdot\mathbf{A}_i\rangle_{xx,0} = \langle\mathbf{A}_i^{\mathrm{T}}\cdot\mathbf{G}_i\cdot\mathbf{A}_i\rangle_{yy,0} = \langle\mathbf{A}_i^{\mathrm{T}}\cdot\mathbf{G}_i\cdot\mathbf{A}_i\rangle_{zz,0} = {}^2/_3G_i^{\perp} + {}^1/_3G_i^{\parallel} \quad (20)$$

Then after simple derivation, we arrive at the results

$$\delta_{xx}{}^2 = \frac{\delta'_{xx}{}^2\sum f_i\langle d_i^2\rangle_0 + \sum f_i\langle P_2(\cos\theta_i)\rangle(G_i^{\perp} - G_i^{\parallel})}{\sum f_i\langle d_i^2\rangle_0 + \sum f_i(2G_i^{\perp} + G_i^{\parallel})} \quad (21a)$$

$$\delta_{zz}{}^2 = \frac{\delta'_{zz}{}^2\sum f_i\langle d_i^2\rangle_0 - 2\sum f_i\langle P_2(\cos\theta_i)\rangle(G_i^{\perp} - G_i^{\parallel})}{\sum f_i\langle d_i^2\rangle_0 + \sum f_i(2G_i^{\perp} + G_i^{\parallel})} \quad (21b)$$

and δ^2, given by eq 6, is

$$\delta^2 = \frac{\delta'^2\sum f_i\langle d_i^2\rangle_0}{\sum f_i\langle d_i^2\rangle_0 + \sum f_i(2G_i^{\perp} + G_i^{\parallel})} \quad (22)$$

It is verified that in the hypothetical case of pointlike elements, the δ's coincide with the δ's.

For completeness, we note that these results include, as a particular case, the situation for a rigid particle (i.e., for a single subunit, $N_s = 1$, $d_1 = 0$, $f_1 = 1$). We have

$$\delta_{xx}{}^2 = \frac{\langle P_2(\cos\theta)\rangle(G^{\perp} - G^{\parallel})}{(2G^{\perp} + G^{\parallel})} \quad (23a)$$

$$\delta_{zz}{}^2 = \frac{-2\langle P_2(\cos\theta)\rangle(G^{\perp} - G^{\parallel})}{(2G^{\perp} + G^{\parallel})} \quad (23b)$$

and $\delta^2 = 0$, as it should be since the rigid particle experiences orientation but no shape deformation.

Scattering, Birefringence, and Dichroism. The changes in the macromolecular shape and size can be experimentally detected as changes in the intensity of scattering. The situation is particularly simple for low-angle scattering. On the basis of the results of Navarro et al.,[28] the change in the scattering form factor due to the presence of an external agent can be written as

$$\frac{P_0(\mathbf{q}) - P(\mathbf{q})}{1 - P_0(\mathbf{q})} = \frac{\langle G\rangle_{\beta\beta} - \langle G\rangle_{\beta\beta,0}}{\langle G\rangle_{\beta\beta,0}} = \delta_{\beta\beta}{}^2 \quad (24)$$

In eq 24, $\mathbf{q}$ is the scattering vector with modulus $q = (4\pi/\lambda)\sin(\theta_s/2)$, where λ is the radiation wavelength and θ_s is the angle subtended by the scattering direction and the prolongation of the incident beam. According to eq 24, $\delta_{\beta\beta}{}^2$ is independent of the scattering angle. We recall that β is the direction perpendicular to the incident beam in the scattering plane. Thus, changing the mutual orientation of the scattering plane and the electric field, the electric-field light-scattering experiment could provide the values for all the $\delta_{\alpha\alpha}{}^2$ and δ^2. As it will become apparent in the presentation of results, the largest deformation is in the direction of the field and will be measured applying the field in the scattering plane, perpendicular to the incident beam.

On the other hand, changes in orientation (and also shape and size) of the macromolecule can be detected as changes in birefringence or dichroism. Following Navarro et al.,[28] the excess birefringence of a macromolecular solution with respect

to that of the pure solvent (normalized to the saturation value) can be written as

$$\Delta n^* = \sum_{i=1}^{N_s} x_i \langle P_2(\cos\theta_i)\rangle \tag{25}$$

In eq 25, x_i is the fraction

$$x_i = \frac{(\gamma_{||} - \gamma_{\perp})_i}{\sum_{i=1}^{N_s}(\gamma_{||} - \gamma_{\perp})_i} \tag{26}$$

with $\gamma_{||,i}$ and $\gamma_{\perp,i}$ being the main components of the polarizability tensor of the ith segment, in directions along the segment axis and perpendicular to it, respectively. One particular case of interest is when all the subunits have a similar elongated structure of identical composition (for instance, helices) and only differ in length. In this case we may take $(\gamma_{||} - \gamma_{\perp})_i \propto L_i$, where L_i is the subunit length. Although eq 25 is particularized for birefringence, we remark that the same treatment can be applied to dichroism, with the extinction tensor, ϵ, playing the role of the optical anisotropy tensor, and if ϵ is axially symmetric, an expression similar to eq 25 will hold for the reduced dichroism.

For a rigid macromolecule

$$\Delta n^* = \langle P_2(\cos\theta)\rangle \tag{27}$$

so that δ_{xx}^2, δ_{zz}^2 and Δn^* are mutually proportional (see eq 23).

Model and Methods

Semiflexible Macromolecules in an Electric Field. The potential energy, V, of a segmentally flexible macromolecule in an electric field will contain two contributions, $V = V_{\text{int}} + V_{\text{elect}}$. The first one, V_{int}, is just the internal energy associated to the deformation of the macromolecule, i.e., to its departure from the most stable configuration. In principle, nothing more can be anticipated about this term.

The second contribution, V_{elect}, gives the interaction energy of the molecule with the electric field and can be expressed as a sum of individual terms, $V_{\text{elect},i}$, corresponding to the various parts or subunits. These terms will depend on the permanent dipoles, μ_i, if they exist, and there may also be a contribution from the induced dipoles determined by the electrical polarizabilities, ϵ_i. When the subunits have revolution symmetry, we assume that μ is along the symmetry axis and that ϵ has parallel and perpendicular components $\epsilon^{||}$ and $\epsilon^{\perp}$. In that case the interaction energy is reduced to a simple form, which contains the modules of the subunit dipoles, μ_i, and polarizability differences $\epsilon_i^{||} - \epsilon_i^{\perp}$, and depends on the angle, θ, subtended by the symmetry axis and the direction of the electric field[1,19]

$$\frac{V_{\text{elect}}}{k_B T} = -\sum_{i=1}^{N_s}(a_i \cos\theta_i + b_i \cos^2\theta_i) \tag{28}$$

where $\cos\theta_i = (\mathbf{E}\cdot\mathbf{u}_i)/E$ is the angle between the electric field and the arm vector. The parameters that describe the intensity of the molecule-field interaction are

$$a_i = \mu_i E/k_B T \tag{29}$$

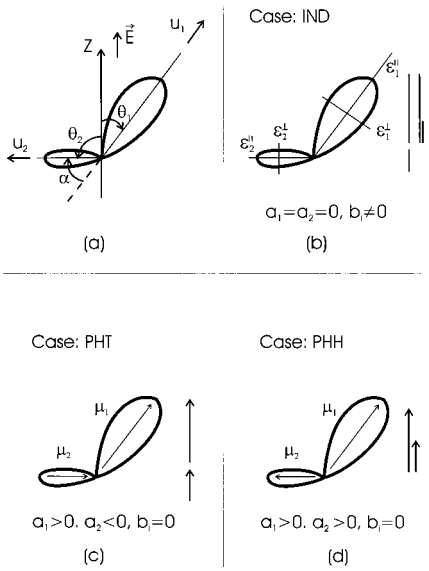

Figure 2. A two-subunit particle. (a) Direction of the arm vectors; Z is the direction of the electric field. (b) Case I with induced dipoles arising form the electrical polarizabilities of the subunits. (c) Case PHT, permanent head-to-tail dipoles. (d) Case PHH, permanent head-to-head dipoles. In the three cases, the orientation of the subunit in an infinitely strong field is indicated.

and

$$b_i = \frac{(\epsilon_i^{||} - \epsilon_i^{\perp})E^2}{2k_B T} \tag{30}$$

Equation 28 allows the representation of permanent and induces dipoles and any hybrid of these two simple types. Some biopolymers may behave according to more complex polarization mechanism; this is for instance the case for DNA.[30] The simple molecule-field interaction mechanisms, based on either permanent or induced dipoles, do not apply to polyelectrolyte systems, particularly at high fields, due to the usual saturation of the polyelectrolyte dipoles. On the other hand, our treatment will be applicable to a variety of macromolecules which clearly possess an important permanent or induced dipoles. Although the presentation in this paper is restricted to the permanent and induced types, we anticipate that the Monte Carlo procedure to be used for the generation of results can be easily applied to an arbitrary molecule-field interaction.

Two-Subunit Model. For the numerical results that we will display later, the model that we consider as representative of segmentally semiflexible macromolecules has two subunits, or arms, whose shape and physical properties have revolution symmetry. This model has been successfully used to study myosin rod,[10,19] and could be applied to other systems like the myosin S1[17] or nucleic acid helices[31] for which segmental flexibility has been proposed, even if it has not been unambiguously demonstrated, at least as an adequate working hypothesis. The two arms are joined by a single joint, as depicted in Figure 2. The main symmetry axes, with unitary vectors $\mathbf{u}_i$ ($i = 1,2$) are defined for each arm, and the instantaneous conformation of the particle is determined by the angle, α, between them. If α_0 is the equilibrium value of this angle, the internal potential energy required for bending or deformation is, for simplicity, assumed to be given by the quadratic form:

$$\frac{V_{\text{int}}}{k_B T} = Q(\alpha - \alpha_0)^2 \tag{31}$$

where k_BT is Boltzmann's factor and Q is the flexibility parameter, with $Q = 0$ for the completely flexible case and $Q \rightarrow \infty$ for the completely rigid one. In various relevant cases, the equilibrium conformation is the straight one, with $\alpha_0 = 0$, but cases with $\alpha_0 \neq 0$ could be also interesting and can be treated in the same way.

The molecule−field interaction is given by eq 28 for symmetric subunits, with $N_s = 2$. A schematic view of the electrical properties is given in Figure 2a. When the permanent dipoles μ_i are nonzero, there are two possibilities for the disposition of the dipoles: head-to-head (PHH) (Figure 2d) and head-to-tail (PHT) (Figure 2c). The electric parameters are $b_i = 0$ for a purely permanent dipole moment and $a_i = 0$ for a purely induced moment (IND). a_i is positive if μ_i is in the same direction as $\mathbf{u}_i$, and negative if it points in the opposite one. For dipoles joined head-to-head, a_1 and a_2 are positive, while for the head-to-tail case we take a_1 positive and a_2 negative.

Monte Carlo (MC) Simulation. Even this simple two-subunit model cannot be treated analytically for arbitrary strong fields. Then, in order to study the conformation of the macromolecule in the presence of the electric field, and concretely for the evaluation of the averages needed for the steady-state molecular shape and birefringence, we employ the same Monte Carlo (MC) procedure used by Iniesta and García de la Torre.[19] The total potential energy of the molecule is given by $V = V_{elect} + V_{int}$, where V_{elect} and V_{int} are given by eqs 28 and 31, respectively. V is a function of the set of polar angles of the arms in the laboratory system, $\{\theta_1, \phi_1, \theta_2, \phi_2\}$, which specifies the orientations of the two-arm vectors, $\mathbf{u_1}$ and $\mathbf{u_2}$.

In the procedure, a new conformation of the particle is obtained from the previous one in the Monte Carlo step by changing the orientation of the arms. This is done adding random increments to cos θ_i and ϕ_i whose maximum absolute values are $\Delta \cos\theta$ and $\Delta\phi$. For the new conformation the total energy is calculated, and the conformation is accepted if $V < V'$, where V' was the energy of the previous conformation. Else, a random number, ρ, uniformly distributed in (0,1) is generated. If $\rho > \exp[(V' - V)/kT]$, the new conformation is accepted; otherwise, it is rejected and the old conformation is counted once again.

For small values of the maximum increments $\Delta \cos\theta$ and $\Delta\phi$, the probability of acceptance is high but the conformational space is scanned slowly due to the smallness of the simulation steps. For high values of the increments the probability of acceptance is low and therefore the scan speed is slow again. The latter is particularly true for high values of the electric field strength or the stiffness constant. Good values of $\Delta \cos\theta$ and $\Delta\phi$ are those for which the probability of acceptance is 10−30%. Example of extreme situations are $\Delta \cos\theta = 0.05$, $\Delta\phi = 1$ for $a^2 + 2b = 2$ and $\Delta \cos\theta = 0.25$, $\Delta\phi = 1$ for $a^2 + 2b = 40$.

Using this procedure, a very large number of conformations (of the order of 10^6−10^7) are generated, and a subset (of typically 10^5) is taken for averaging.

Numerical Results and Discussion

The application of an electric field of a certain intensity during a time long enough to reach steady state will produce two main effects in flexible macromolecule: orientation according to the field and deformation respect to the field-free conformation. The conformational changes (overall deformation) will be seen as changes in $\langle s^2 \rangle$, while the changes in birefringence and the components of $\langle \mathbf{G} \rangle$ will reflect both orientation and deformation of the semiflexible particle. Hereafter, we analyze these three phenomena.

For the numerical calculation and presentation of results, we consider the case of a segmentally flexible macromolecule with two identical subunits with cylindrical symmetry. It seems clear that the effects of flexibility on the properties are larger when the subunits are identical or of similar sizes than when one is much larger than the other one. The straight conformation is considered to be most stable, so that $\alpha_0 = 0$. No further specifications have to be made for the calculation of the normalized birefringence according to eq 25. For the calculation of gyration tensor and deformation, one has to specify the size and shape of the subunits. Then, we have chosen a paradigmatic example of segmentally flexible macromolecular model, namely the once-broken rod. There are several biological macromolecules or supramolecular complexes that are described by this model, such as the myosin fragment known as myosin rod,[10,32] for which a value of about $Q = 0.5$ has been reported.[10,19] For simplicity we assume that the hinge is at the middle, so that the two arms are identical. As it happens with myosin rod, the diameter of the arms is much smaller than their length, and therefore we use the equations for axially symmetric subunits, with $G_i^{||} = 0$, while $G_1^{\perp} = G_2^{\perp} = (L/2)^2/24$, where $L/2$ is the length of each arm.

Birefringence. Monte Carlo results for the birefringence of segmentally flexible particles with two identical subunits ($|a_1| = |a_2|$, $b_1 = b_2$) and a straight equilibrium conformation ($\alpha_0 = 0$) are shown in Figure 3. According to the Kerr law, the birefringence at very low fields is proportional to $a_i^2 + 2b_i$, i.e., to the squared field intensity, E^2. In the Kerr region, the simulations are difficult because the birefringence is very small and therefore statistical uncertainties are important in relative terms. Anyhow, the proportionality between Δn and $a_i^2 + 2b_i$ (slope = 1 in a log−log plot) is noticed in Figure 3B. For a very stiff rod, the results must converge to those of a straight rod with $a = 2a_i$, $b = 2b_i$. For this special case analytical results are available[1] for the purely induced and purely permanent head-to-tail dipole moments.

Analysis of Figure 3 reveals some interesting features. Thus, for the completely flexible particle, with $Q = 0$, the birefringence is the same for the two dipole types, PHT and PHH, while this degeneration disappears when Q increases. The reason is that for $Q = 0$, the two arms can respond to the application of the field independently of each other, while for nonzero Q their orientations are correlated, in different ways for the PHT and PHH cases.

When the macromolecule is nearly rigid ($Q = \infty$), with PHT dipoles, an increase in the field produces a higher orientation and consequently an increase in Δn^*, but for PHH at low fields (when the PHT and IND cases present an appreciable value of Δn^*), the molecules are not oriented ($\Delta n^* \approx 0$). The reason is that unless the macromolecule is not sufficiently deformed the two PHH dipoles are nearly collinear and cancel each other. For the completely flexible case ($Q = 0$) the interesting feature is that the PHT and PHH cases give the same birefringence (indeed this can be theoretically reasoned). In general, Figure 3 illustrates the trend followed by the birefringence as the parameter Q is varied.

In general, our results for the electric birefringence of the two-subunit particle confirm, now with much better statistical quality, the results of the previous study of the birefringence by Iniesta and García de la Torre,[19] where the reader is referred for further details.

Deformation. The amount of pure deformation (not including orientational effects) can be analyzed in the statistics of the angle between the two subunits. If $\mathbf{v}_1$ and $\mathbf{v}_2$ are the vectors from the

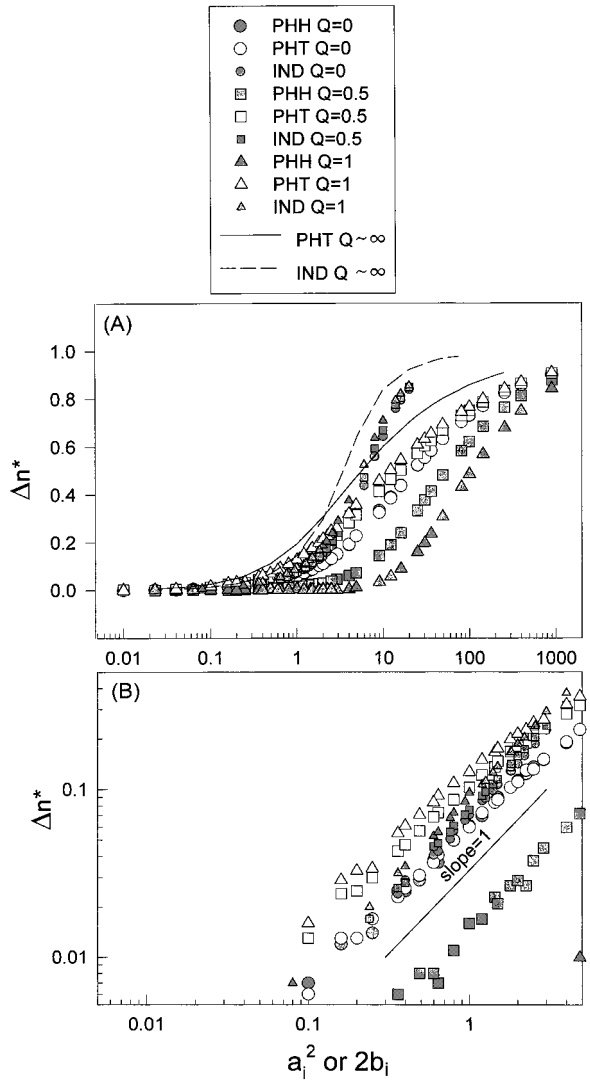

Figure 3. Normalized birefringence of two-subunit particle with $\alpha_0 = 0$, various values of Q, and three types of molecule−field interaction. (A) Results for a wide range of field strengths. (B) Results for low fields, in the Kerr region.

hinge to the subunit centers of mass, then the center-to-center distance is $r_{12} = \mathbf{v}_1^2 + \mathbf{v}_2^2 + 2\mathbf{v}_1\mathbf{v}_2 \cos\alpha$. From eq 13, it follows that

$$\langle s^2\rangle - \langle s^2\rangle_0 = f_1 f_2 \upsilon_1 \upsilon_2 (\langle\cos\alpha\rangle - \langle\cos\alpha\rangle_0) \qquad (32)$$

This result is general for any two-subunit macromolecule, with the only restriction that α should be defined as the angle subtended by vectors $\mathbf{v}_1$ and $\mathbf{v}_2$. $\langle\cos\alpha\rangle_0$ is determined by the (field-off) flexibility of the particle and will depend on Q, while $\langle\cos\alpha\rangle$ will depend also on the electric parameters. Thus from results of $\langle\cos\alpha\rangle$ as a function of Q, a_i and b_i, the absolute increase in the radius of gyration, formulated in eq 32 can be evaluated.

For two identical subunits, $\upsilon_1 = \upsilon_2 = \upsilon$ and

$$\langle s^2\rangle - \langle s^2\rangle_0 = (1/4)\upsilon^2(\langle\cos\alpha\rangle - \langle\cos\alpha\rangle_0) \qquad (33)$$

In this case, we have evaluated from the Monte Carlo simulation $\langle\cos\alpha\rangle$. The results are displayed in Figure 4.

Although the change in the overall radius of gyration is determined by $\langle\cos\alpha\rangle$, this quantity is not sufficient to characterize the deformation process; rather, we may regard the

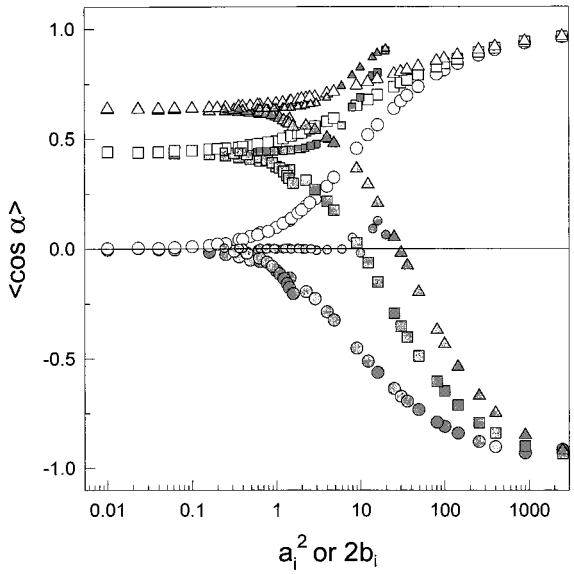

Figure 4. $\langle\cos\alpha\rangle$ for a two-subunit particle with identical arms, and $\alpha_0 = 0$. Symbols are as in Figure 3.

effects of the field on the distribution of angles, $P(\alpha)$, which can readily be obtained from the Monte Carlo simulations. Figure 5 shows histograms of this distribution in the case of the completely flexible particle ($Q = 0$). In the absence of field, the distribution is uniform, with $P(\alpha) = \sin(\alpha)/2$, and $\langle\cos\alpha\rangle_0 = 0$. When field is applied to a particle with PHT dipoles, the particle is straightened by the field, with conformations with smaller α being favored, and the peak in $P(\alpha)$ moves to the left. Conversely, if the dipoles were PHH, the peak will move to greater α; in both cases the distribution becomes asymmetric. As a consequence, in Figure 4 we see how in the former case, $\langle\cos\alpha\rangle$ decreases below $\langle\cos\alpha\rangle_0$ while in the latter cases it increases. However, the situation for IND dipoles is very peculiar. For $Q = 0$ and any value of b_i, the probability of any angle and that of its supplementary is identical, i.e., $P(\alpha) = P(\pi-\alpha)$, so that the distribution is bimodal and symmetric. The average remains $\langle\cos\alpha\rangle = 0$ for any value of the field intensity, and the consequence is that the overall radius of gyration does not change in the presence of the field. Indeed, this is shown by the numerical results in Figure 4, although we observe a departure from this prediction at high field (say, for $b > 3$). The reason is that at higher fields, the potential barrier that separates the conformations with $\alpha \approx 0$ and $\alpha \approx \pi$ is very high, so that during the simulation the particle there are few transitions between one and the other extremes and the results are biased. For a partially flexible particle, the symmetry is broken, but the distribution is still bimodal, particularly at intense fields. In Figure 4 we see that there is a slight variation of $\langle\cos\alpha\rangle$ with field strength, but much weaker than that for permanent dipoles.

We note that the results and discussion presented so far, for Δn, $\langle\cos\alpha\rangle$, and $\langle s^2\rangle - \langle s^2\rangle_0$, are independent of shape details, being valid for any two-subunit particle with identical, axially symmetric subunits. If we wish to evaluate relative deformation, as indicated by the δ^2 parameters, the specific shape of the subunits has to be accounted for and, as commented above, we have chosen the example of the long, thin rod. Results for δ^2 are shown in Figure 6, where we also include the deformation parameters for the *xx* and *zz* components of the gyration tensor. As for the preceding properties, results are shown for the three dipole types and various values of Q. The case of $Q \rightarrow \infty$ can be easily predicted from the results for the single, rigid, axially symmetric particle; if we have, as for the long rod, $G^{\parallel} \gg G^{\perp}$,

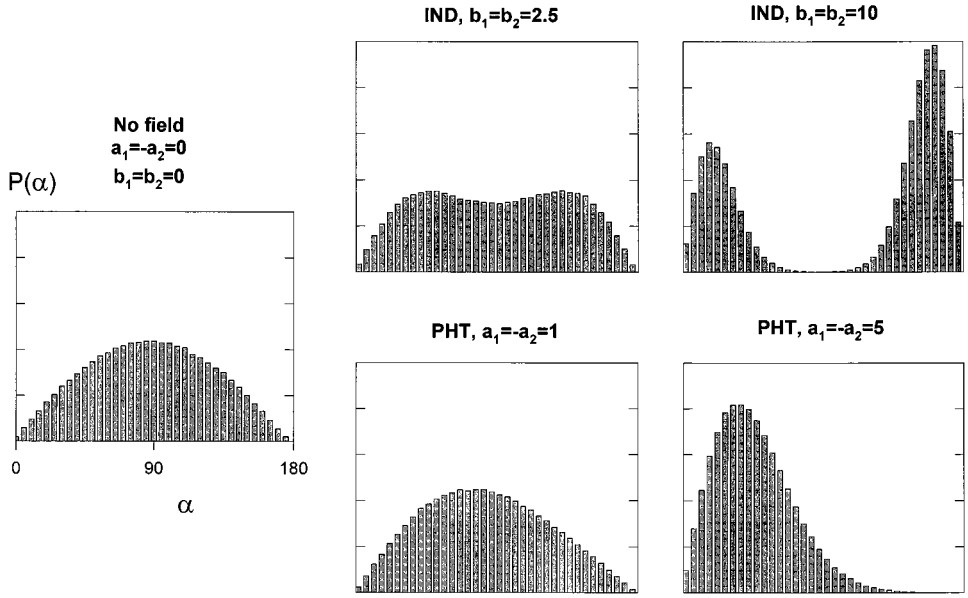

Figure 5. Distribution $P(\alpha)$ for a completely flexible ($Q = 0$) two-subunit particle with identical arms, with $\alpha_0 = 0$. Results in the absence of field, for PHT dipoles, and for IND dipoles.

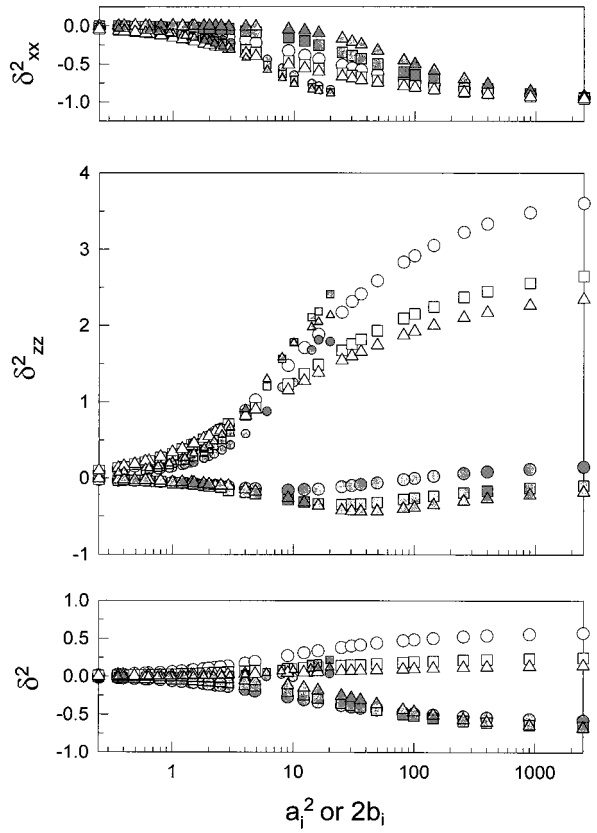

Figure 6. Deformation parameters, δ^2, for the *xx* and *zz* components of the gyration tensor and for the radius of gyration. The particle is a broken rod with very long and thin arms, with $\alpha_0 = 0$. Symbols are as in Figure 3.

then eqs 23 reduce to the relationships $\delta_{xx}^2 = \delta_{zz}^2/2 = \Delta n^* = \langle P_2(\cos\theta)\rangle$, with overall deformation $\delta^2 = 0$ as it is obvious for a rigid, undeformable particle.

If we look at the scales of the ordinate axes in the plots in Figure 6, we can appreciate the different behavior and sensitivity of $\langle G\rangle_{xx}$, $\langle G\rangle_{zz}$, and $\langle s^2\rangle$, or their corresponding parameters, δ_{xx}^2, δ_{zz}^2, and δ^2, to the field strength. For all the dipole types, $\langle G\rangle_{xx}$ goes from its field-free value, $\langle G\rangle_{xx,0}$, to zero, and correspondingly δ_{xx}^2 goes from 0 to -1. If the δ_{xx}^2 results are superimposed (not shown) on to those of $-\Delta n^*$, with a change of sign, one immediately observes that not only the trends of the points but also even the numerical values are rather similar. The information provided by Δn^* and δ_{xx}^2, or in other words, by electric birefringence and by electric-field light scattering with a horizontal scattering plane, are roughly equivalent. A separate question, in which we do not enter, is which of the two techniques is experimentally more feasible.

In Figure 6 we also show the plot corresponding to the $\langle G\rangle_{zz}$ component that is observed in electric-field light scattering with a vertical scattering plane. We notice the remarkably high values of δ_{xx}^2 reached at high fields for the PHT and IND dipole types, which indicate an up to 5-fold increase in $\langle G\rangle_{zz}$. Furthermore, for the PHH dipoles, δ_{xx}^2 is rather different: negative and much smaller in absolute value. This is in contrast with the trend of the δ_{zz}^2 and Δn^*, which is qualitatively similar for the three dipole cases. Thus, δ_{xx}^2 seems to provide a better criterion to ascertain, from electric-field light scattering, the arrangement of the subunit dipoles in the segmentally flexible macromolecule. Finally, in Figure 6 we also show the values of δ^2, corresponding to the expansion in the overall radius of gyration. Here, we note a different sign depending on the dipole type, although the absolute values are moderate.

As commented previously, the electric birefringence can be studied at low fields, where Δn is proportional to E^2. Particularly, for a rodlike molecule, $\Delta n \propto (a^2 + 2b)$ where a and b are given by eqs 29 and 30. For a broken rod of equal arms, we have $\Delta n \propto (a_i^2 + 2b_i)$, or $\Delta n \propto a_i^2$ for PHH and PHT, and $\Delta n \propto 2b_i$ for IND dipoles (this has been indeed verified by Iniesta and García de la Torre[19]). In a log−log plot of Δn vs a_i^2 or $2b_i$, the slope must be 1. It is pertinent to recall the above-commented difficulty for simulations at low field. Anyhow, our results in Figure 7 show how this prediction is reasonably well obeyed by the three deformation parameters, so that these deformations are also proportional to E^2.

Although for some of the results we have specified the example of the long, centrally hinged rod, it is clear that the numerical procedure is applicable to any other two-subunit particle. Furthermore, in our theoretical framework no limitation has been included relative to the number of subunits, which

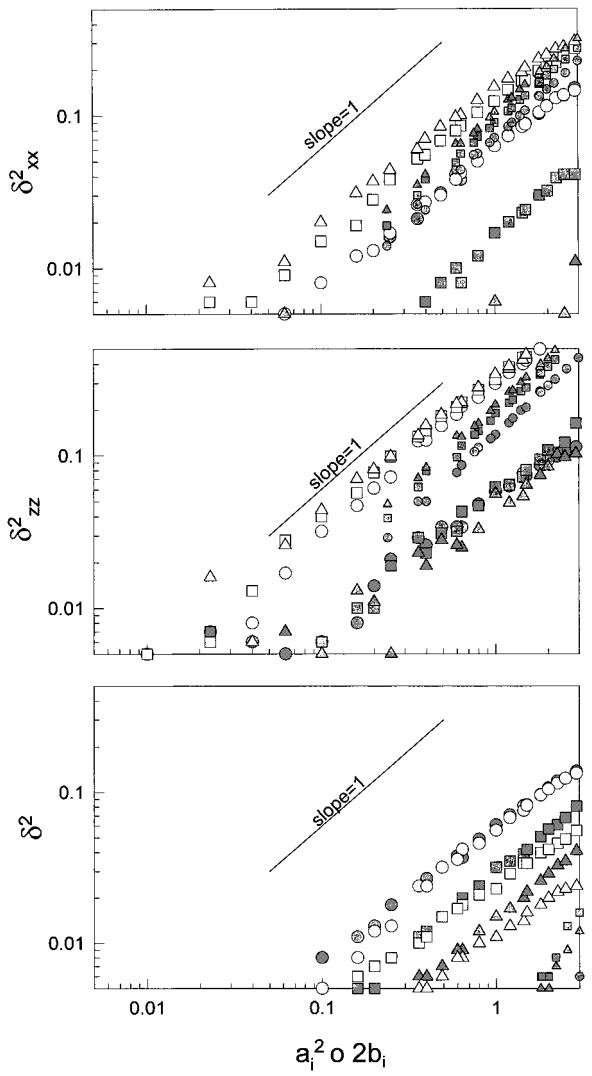

Figure 7. log−log plot of deformation parameters vs a_i^2 or $2b_i$. The slope = 1 indicates that these deformations are proportional to E^2.

means that identical treatment can be formulated for any N_s, and the Monte Carlo procedure can be easily implemented in any case.

Acknowledgment. This work has been funded by grant PB96-1106 and a predoctoral fellowship to B.C., both from the Dirección General de Enseñanza Superior (M.E.C.), and grant 01758/CV/98 from Fundación Séneca (C.A.R.M.).

References and Notes

(1) Frederick, E.; Houssier, C. *Electric Dichroism and Electric Birefringence*; Clarendon Press: Oxford, U.K., 1973.

(2) Riande, E.; Saiz, E. *Dipole Moments and Birefringence of Polymers*; Prentice Hall; Englewood Cliffs: NJ, 1992.

(3) Holcomb, D. N.; Tinoco, I. J. *J. Phys. Chem.* **1963**, *67*, 2691.

(4) Wegener, R. M.; Dowben, R. M.; Koester, V. J. *J. Chem. Phys.* **1979**, *70*, 622.

(5) García de la Torre, J.; Bloomfield, V. A. *Q. Rev. Biophys.* **1981**, *14*, 81.

(6) García de la Torre, J. Rotational diffusion coefficients. In *Molecular Electrooptics*; Krause, S., Ed.; Plenum Publishing Corp.: New York, 1981; p 75.

(7) García de la Torre, J. Hydrodynamic Properties of Macromolecular Assemblies. In *Dynamic Properties of Macromolecular Assemblies*; Harding, S. E., Rowe, A. J., Eds.; The Royal Society of Chemistry: London, 1989; p 3.

(8) Yguerabide, J.; Epstein, H. F.; Stryer, L. *J. Mol. Biol.* **1970**, *51*, 573.

(9) Harvey, S. C.; Cheung, H. *Myosin Flexibility, in Cell and Muscle Motility*; Dowben, R. M., Shay J. W., Eds; Plenum: New York, 1982; Vol. 2, p 279.

(10) Iniesta, A.; Díaz, F. G.; García de la Torre, J. *J. Biophys.* **1988**, *54*, 269.

(11) Matsumoto, T.; Nishioka, N.; Teramoto, A.; Fujita, H. *Macromolecules* **1975**, *7*, 824.

(12) Muroaga, Y.; Tagawa, H.; Hiragi, Y.; Ueki, T.; Kataoka, M.; Izuni, Y.; Aneniya, Y. *Macromolecules* **1988**, *21*, 2760.

(13) García de la Torre, J.; Bloomfield, V. A. *Biochemistry* **1980**, *19*, 5118.

(14) Rau, D. C.; Ganguly, C.; Korn, E. D. *J. Biol. Chem.* **1993**, *268*, 4612.

(15) Rau, D. C. *J. Biol. Chem.* **1993**, *268*, 4622.

(16) Burton, D. F. Structure and function of antibodies. In *Molecular Genetics of Immunoglobulin*; Calabi, F., Neuberger, M. S., Eds.; Elsevier: 1987; p 1.

(17) Eden, D.; Highsmith, S. *Biophys. J.* **1997**, *73*, 952.

(18) Mellado, P.; García de la Torre, J. *Biopolymers* **1982**, *21*, 1857.

(19) Iniesta, A.; García de la Torre, J. *J. Chem. Phys.* **1989**, *90*, 5190.

(20) Jennings, B. R. Light scattering in electric fields. In *Molecular Electrooptics*; Krause, S., Ed; Plenum Publishing Corporation: New York, 1981; p 181.

(21) Khanarian, G.; Stein, R. S. *Macromolecules* **1987**, *20*, 2858.

(22) Heller, W. *J. Chem. Phys.* **1982**, *76*, 69.

(23) Link, A.; Springer, J. *Macromolecules* **1993**, *26*, 464.

(24) Porschke, D. *Biopolymers* **1989**, *28*, 1383.

(25) Harvey, S. C.; Mellado, P.; García de la Torre, J. *J. Chem. Phys.* **1983**, *78*, 2081.

(26) García de la Torre, J. *Eur. Biophys. J.* **1994**, *23*, 307.

(27) Sólvez, J. A.; Iniesta, A.; García de la Torre, *J. Int. J. Biol. Macromol.* **1988**, *9*, 39.

(28) Navarro, S.; Carrasco, B.; López Martínez, M. C.; García de la Torre, J. *Int. J. Polym. Sci. B: Polym. Phys.* **1997**, *35*, 689.

(29) López Cascales, J. J.; Navarro, S.; García de la Torre, J. *Macromolecules* **1992**, *25*, 3574.

(30) Porschke, D. *Biophys. Chem.* **1985**, *22*, 237.

(31) Vacano, E. and Hagerman, P. J. *Biophys. J.* **1997**, *73*, 306.

(32) Hvidt, S.; Chang, T.; Yu, H. *Biopolymers* **1984**, *23*, 1283.